




# Histone H3.3 chaperone HIRA renders stress-responsive genes poised for prospective lethal stresses in acquired tolerance

Yoshikazu Nagagaki<sup>1</sup>  | Yuji Kozakura<sup>1</sup> | Theventhiran Mahandaran<sup>1</sup>  |  
Yukiko Fumoto<sup>1</sup> | Ryuichiro Nakato<sup>2</sup> | Katsuhiko Shirahige<sup>2</sup> |  
Fuyuki Ishikawa<sup>1,3</sup> 

<sup>1</sup>Department of Gene Mechanisms, Graduate School of Biostudies, Kyoto University, Kyoto, Japan

<sup>2</sup>Laboratory of Genome Structure and Function, Institute for Quantitative Biosciences, The University of Tokyo, Tokyo, Japan

<sup>3</sup>Radiation Biology Center, Graduate School of Biostudies, Kyoto University, Kyoto, Japan

## Correspondence

Fuyuki Ishikawa, Kyoto University, Graduate School of Biostudies and Research Administration Center (KURA), Yoshida-Honmachi, Sakyo-ku, Kyoto, 606-8501, Japan.

Email: [ishikawa.fuyuki.7u@kyoto-u.ac.jp](mailto:ishikawa.fuyuki.7u@kyoto-u.ac.jp)

## Funding information

Uehara Memorial Foundation, Grant/Award Number: 202220433; Japan Agency for Medical Research and Development, Grant/Award Number: 21cm0106113h0006; Japan Society for the Promotion of Science, Grant/Award Numbers: 14J08310, 15H02383, 25134710, JPJSCCA20200009

Communicated by: Yasushi Hiraoka

## Abstract

Appropriate responses to environmental challenges are imperative for the survival of all living organisms. Exposure to low-dose stresses is recognized to yield increased cellular fitness, a phenomenon termed hormesis. However, our molecular understanding of how cells respond to low-dose stress remains profoundly limited. Here we report that histone variant H3.3-specific chaperone, HIRA, is required for acquired tolerance, where low-dose heat stress exposure confers resistance to subsequent lethal heat stress. We found that human HIRA activates stress-responsive genes, including *HSP70*, by depositing histone H3.3 following low-dose stresses. These genes are also marked with histone H3 Lys-4 trimethylation and H3 Lys-9 acetylation, both active chromatin markers. Moreover, depletion of HIRA greatly diminished acquired tolerance, both in normal diploid fibroblasts and in HeLa cells. Collectively, our study revealed that HIRA is required for eliciting adaptive stress responses under environmental fluctuations and is a master regulator of stress tolerance.

## KEYWORDS

acquired tolerance, Chromatin remodeling, heat shock protein, HIRA, histone chaperone, histone H3.3, hormesis, stress response

## 1 | INTRODUCTION

Widely observed in various contexts, in organisms and cells across species and kingdoms, low-dose stress can be beneficial, whereas high-dose stress inflicts harm. The

pro-survival effects elicited by weak stresses are collectively called hormesis (Calabrese et al., 2011). One type of hormesis, acquired tolerance, occurs when exposure to mild stress (priming stress) results in the acquisition of stress resistance to a subsequent severe stress which

This is an open access article under the terms of the [Creative Commons Attribution-NonCommercial](https://creativecommons.org/licenses/by-nc/4.0/) License, which permits use, distribution and reproduction in any medium, provided the original work is properly cited and is not used for commercial purposes.

© 2024 The Author(s). *Genes to Cells* published by Molecular Biology Society of Japan and John Wiley & Sons Australia, Ltd.

would otherwise be lethal (lethal stress). It has long been recognized that mild ischemia induces resistance to subsequent profound ischemia in the heart and brain; this is called post-conditioning tolerance (reviewed in [Dirnagl et al., 2009; Heusch, 2013]), representing a form of acquired tolerance. Acquired tolerance has been observed with various combinations of different priming and lethal stresses, not only ischemia. The anti-aging effect of caloric restriction is arguably a hormetic effect brought about by mild starvation (reviewed in [Gems & Partridge, 2008]). Notably, it is known that cancer cells experience ever-changing mild stresses from microenvironments (Gillies et al., 2012). As such, acquired tolerance appears to be a fundamental reaction that enhances organismal survival in a changeable environment.

Histone H3.3 is produced constitutively throughout the cell cycle and non-proliferating conditions, while the canonical H3 histones, H3.1 and H3.2, are produced specifically in S phase of proliferating cells. H3.3 differs from H3.1 and H3.2 by five and four amino-acid substitutions, respectively. Nevertheless, H3.3 is a unique chromatin marker deposited in a diverse range of cellular contexts (Ahmad & Henikoff, 2002; Pchelintsev et al., 2013). Incorporation of H3.3 into transcriptionally active chromatin is mediated by the histone chaperone complex HIRA (Goldberg et al., 2010; Ray-Gallet et al., 2002; Tagami et al., 2004). We previously found by a genetic screen in *Schizosaccharomyces pombe* that fission yeast HIRA is required for acquired tolerance (Chujo et al., 2012; Tarumoto et al., 2013). Mild priming stresses facilitate the transcription of stress-responsive genes via HIRA-mediated chromatin remodeling, thereby conferring tolerance to subsequent lethal stress. Here we explored whether human HIRA is required for acquired tolerance in human cells. Furthermore, we investigated the mechanism of the low-dose stress response by interrogating global localization of HIRA and histone H3.3 by ChIP-seq and conducting subsequent bioinformatic analyses.

## 2 | RESULTS

### 2.1 | Low-dose heat treatment prior to a lethal dose rescues human cell viability via HIRA

Given that HIRA is conserved from yeast to humans (Kirov et al., 1998), we examined whether HIRA is involved in acquired tolerance in human cells. Immortalized WI-38 normal human fibroblast (WI-38-hTERT) cells were treated with lethal heat stress (47°C, 35 min) with or without a preceding low-dose (priming) stress

(40°C, 2 h), and assayed for viability at 48 h after the lethal stress (Figure 1a). While priming stress alone had no effect on viability, the lethal stress alone decreased cell viability to below 25% compared to control (no stress) cells. However, if the lethal stress was applied immediately after the priming stress, the cell viability was significantly improved to more than 50% (Figure 1b). Similar results were observed in other human cell lines, including primary WI-38, normal primary IMR-90, and HeLa cancer cells (Figure 1c–e). We concluded that mild heat stress elicits acquired tolerance in normal human cells as well as cancer cells. The mammalian HIRA complex consists of three subunits, HIRA, UBN1, and CABIN1 (Rai et al., 2011). shRNA-mediated *HIRA* knockdown had minimal adverse effects on the cellular growth and transcripts under normal culture conditions (fold expression changes between control and *HIRA* knockdown cells of individual genes, including *HIRA*, are shown in Figure S1). However, it significantly impaired acquired tolerance compared to the control cells (Figures 1f, S1b,c), indicating that HIRA is essential for acquired tolerance in human cells.

### 2.2 | Priming mild heat stress activates HIRA-dependent H3.3 deposition throughout the genome, especially at stress-responsive genes

To investigate the role of HIRA in stressed cells, we examined genome-wide endogenous HIRA localization by ChIP-seq using WI-38-hTERT cells harvested immediately after priming stress and non-stressed control cells. The anti-HIRA antibody used for ChIP-seq was raised in our laboratory, and its specificity was demonstrated in immunoblotting experiments (Figure S2). Analysis of the sequence reads aligned on the human reference genome yielded 29,022 peaks with priming stress-treated cells (priming stress) and 19,285 with the unstressed (no stress) cells. To validate our HIRA ChIP-seq results, the sequence reads from the non-stressed sample were compared with those from the published HIRA ChIP-seq data in IMR-90 human normal fibroblasts, which were cultured in low oxygen (3%) (Rai et al., 2014). Despite the differences in cell lines and the culture conditions, the two sets of HIRA ChIP-seq data showed moderate correlations in distributions and intensities of the peaks over the genome ( $r = 0.50$ ; Figure S3a). Moreover, to evaluate whether our HIRA peaks were more likely to overlap with those in Rai et al. (Rai et al., 2014) than expected, we generated simulated groups of HIRA peaks by shuffling the peaks from Rai et al. randomly across the genome (randomization test). The results revealed

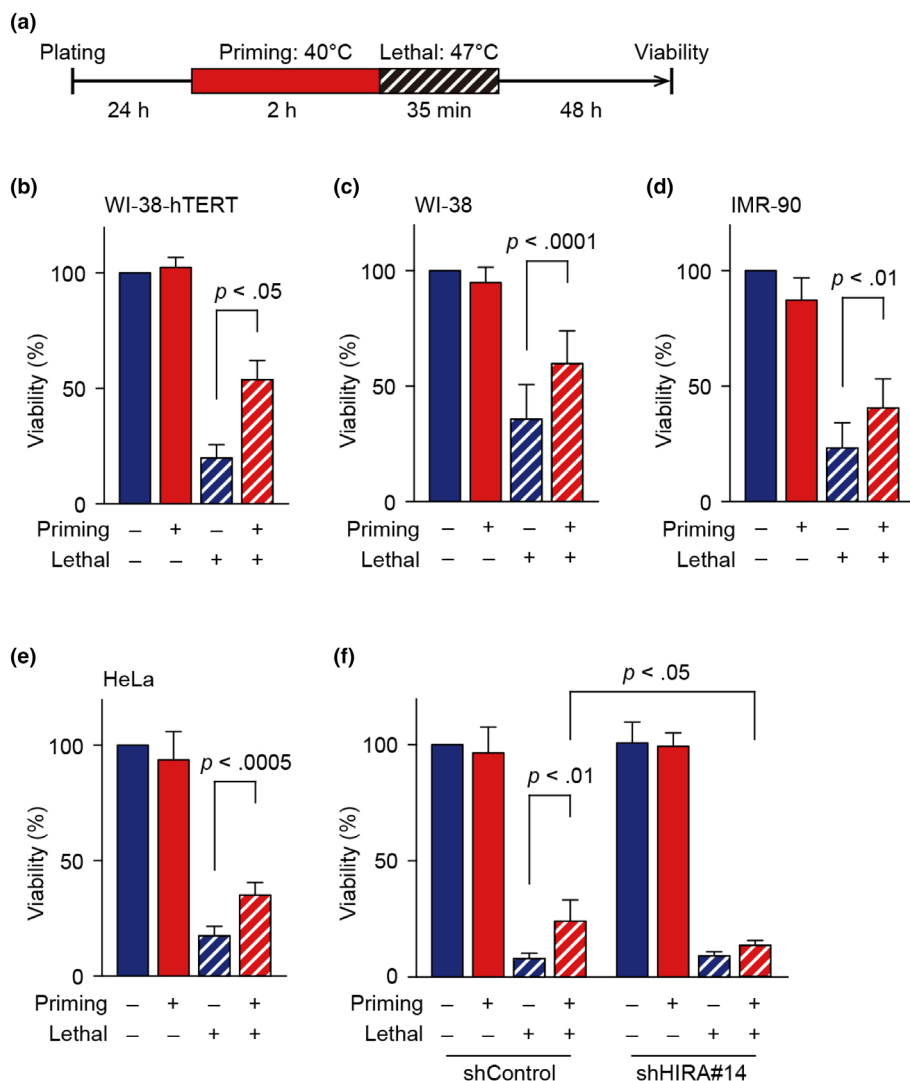


**FIGURE 1** Histone chaperone HIRA is required for acquired tolerance in human cells. (a) Scheme of the acquired tolerance assay. Cell viability was measured two days after stress treatments. (b–f) Viability of normal WI-38-hTERT (b), primary WI-38 (c), IMR-90 (d), HeLa (e) and HIRA knockdown WI-38-hTERT (f) cells in the acquired tolerance assay. Data are presented as mean  $\pm$  S.D. from three independent experiments. A paired two-tailed *t*-test was applied for the statistical analysis.

that the observed overlaps between our HIRA peaks and the reported peaks of Rai et al. (Figure S3b) displayed a significantly higher occurrence ( $p < 2.2e-16$ , Fisher's exact test) when compared to the overlaps between our peaks and the simulated random peaks (Figure S3c). These results suggested that our HIRA ChIP-seq data were reliable enough for further analysis.

The comparisons of peak distributions and intensities between no stress and priming stress samples are displayed as a Venn diagram and MA-plots (Figures 2a,b and S4a–c). While 58% (16,886 out of 29,022) of HIRA-binding sites in primed cells overlapped with those in non-stressed cells, 42% (12,136 out of 29,022) were unique to primed cells, suggesting that HIRA gained de novo binding sites after the priming stress. Despite the different numbers of peaks found in the primed and non-stressed samples, the peaks were located similarly: in both cases, approximately two-thirds of the HIRA peaks corresponded to genic regions (defined as the 5' UTR to the 3'UTR of protein-coding genes), whereas the

remaining third corresponded to intergenic regions (Figure 2c). We analyzed HIRA read frequencies across all protein-coding genes and found that HIRA was particularly enriched at transcription start sites (TSSs) in both stressed and non-stressed conditions (Figure 2d). We also conducted ChIP-seq of histone H3.3 with a histone variant H3.3-specific antibody using WI-38-hTERT cells harvested immediately after priming stress and non-stressed control cells. The antibody's specificity is shown in Figure S5. We found that histone H3.3 was enriched in the vicinity of the HIRA peaks in both primed and non-stressed cells (Figure 2e). Note that the amount of bound H3.3 was less at the very peak of HIRA binding, which corresponded to TSSs, compared to the surrounding regions, likely reflecting the formation of a nucleosome-depleted region at the active promoter, which potentiates transcription (reviewed in [Lorch & Kornberg, 2015]). These data suggested that HIRA functions as a histone chaperone and deposits H3.3 largely in the vicinity of TSSs of genes throughout the genome

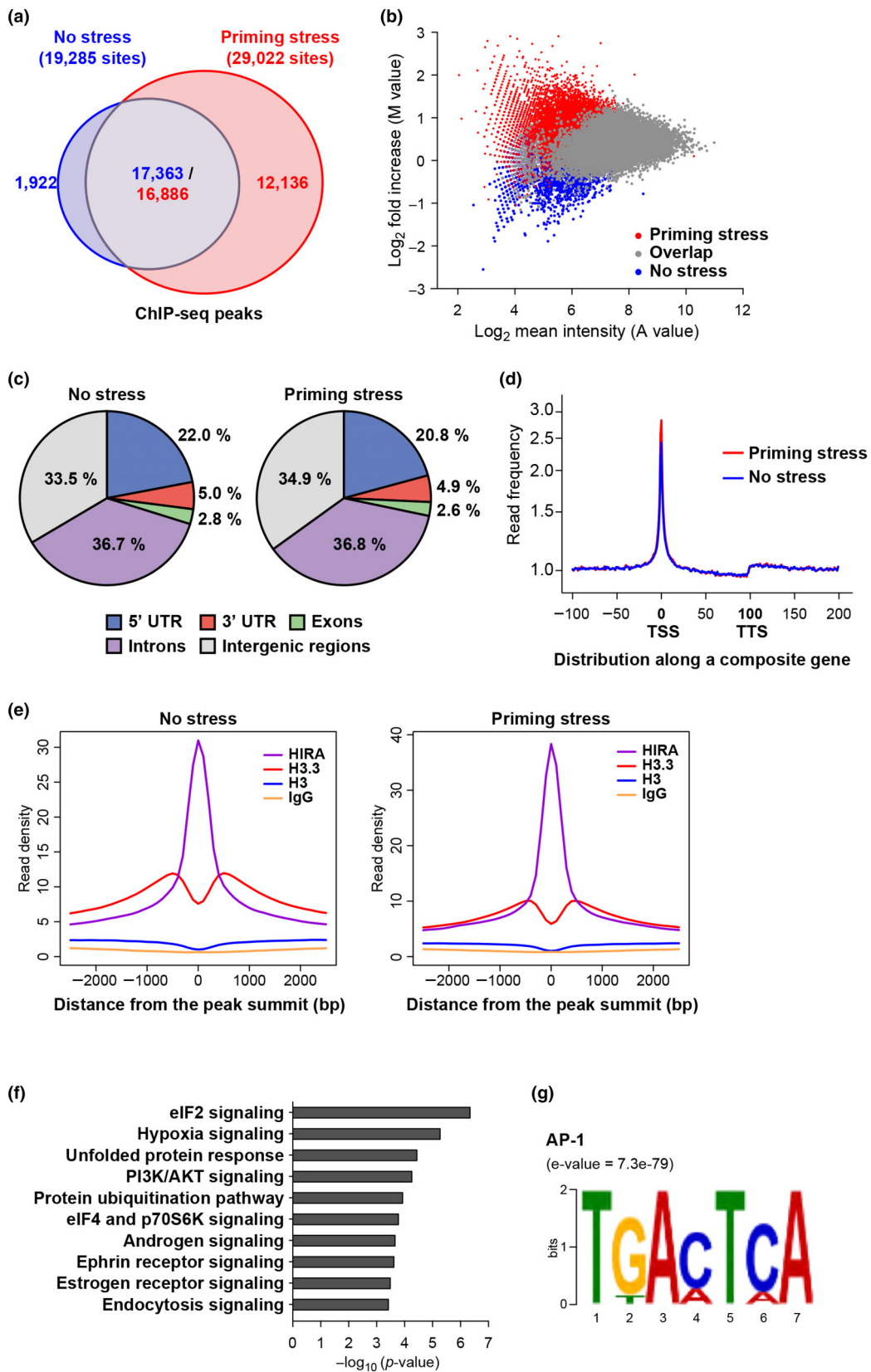


FIGURE 2 Legend on next page.

under low-dose stressed conditions, as is the case in non-stressed conditions.

Pathway analysis of the priming stress-specific HIRA-bound genes revealed that HIRA was enriched in primed cells specifically at genes related to a variety of stress response processes, including translational control, hypoxia signaling, the unfolded protein response, and the ubiquitination pathway (Figure 2f), whereas it was not in non-stressed cells (Figure S4d). Moreover, RNA-seq analysis for the same set of cells identified 455 genes that were upregulated in the priming stress-treated cells. Among them, *HSPA1A*, *HSPA1B*, *HSPA5*, *HSPA6*, *HSPA4L*, *HSPH1* (encoding Hsp70 Members 1A, 1B, 5, 6, 4 Like, and Hsp110, respectively), *DDIT3* (DNA Damage Inducible Transcript 3, alternatively called *GADD153* or *CHOP*, encoding a transcription factor involved in ER stress), *HERPUD1* (*Homocysteine Inducible ER Protein With Ubiquitin-Like Domain 1*, involved in ER quality control), and *DNAJB1* (encoding DnaJ (Hsp40) Member B1) were most highly upregulated (Figure S6a). It is noteworthy that they are all involved in the unfolded protein response (Figure S6b). Furthermore, *HSPA1A*, *HSPA1B*, and *HSPA5* were among the top hits in the gene list of increased HIRA occupancy in the HIRA ChIP-seq experiment (Figure S4a), supporting the causative role of HIRA in upregulating the stress-responsive genes. Totally 379 genes were shown to be downregulated after priming stress (Figure S6a), and it seemed unlikely that they were highly related to a specific pathway (high False Discovery Rates (FDRs), Figure S6c). In addition, sequence motif analysis (see Materials and Methods) revealed that the transcription factor AP-1 binding motif was significantly present among the HIRA-binding sites (Figure 2g). AP-1 is a transcription factor that is activated by a variety of stimuli via stress-activated protein kinase (JNK/SAPK) and regulates the expression of stress-responsive genes. Importantly, a previous study showed that HIRA physically interacts with c-Jun, a component of the AP-1 heterodimer (Pchelintsev et al., 2013). These results suggest that, upon priming stress, HIRA localizes and deposits histone H3.3 at stress-responsive genes to

form a transcriptionally primed chromatin state for a robust defense against prospective severe stresses.

We compared the lists of HIRA-binding genes (Figure 2f) and of the transcriptionally upregulated genes (Figure S6b) after exposure to the priming heat stress. We noticed that the two top-ranked gene groups annotated as the eIF2 signaling and hypoxia signaling pathways were identified in the HIRA-binding gene list, but not in the upregulated gene list. It has been reported that HIRA associates with not only active genes, but also inactive and/or poised genes including those known as bivalent genes (Banaszynski et al., 2013; Jin & Felsenfeld, 2006). We speculate that the translation-regulating eIF2 signaling and hypoxia-responding genes are poised in a HIRA-dependent manner, but not yet activated upon the priming heat stress. These poised states may contribute to the cell survival through quick gene activation once prospective severe stresses happen. Future study is necessary to test this possibility.

### 2.3 | Low-dose stress poises heat shock gene loci for enhanced inducibility upon subsequent lethal heat stress

One of the genomic loci showing profound enrichment of HIRA after priming stress was the TSS and the ORF of *HSPA1A*, which encodes Heat Shock Protein 70 (Figures 3a–c and S4a). Additionally, RNA-seq results showed that *HSPA1A* was one of the most highly upregulated and highly expressed genes upon priming stress exposure (Figure S6a). In contrast, no significant change in HIRA enrichment was observed at *GAPDH* regions (Figure S7a,b). We analyzed chromatin dynamics at the *HSPA1A* locus in detail after the priming stress. Consistent with HIRA recruitment, we observed a trend of histone H3.3 deposition after the priming stress ( $p = 0.054$ ; Figures 3d, and S8a), whereas H3.3 enrichment at *GAPDH* regions was not significantly increased in primed cells compared to non-stressed cells (Figure S7c). Note that the total H3 amount at the *HSPA1A* TSS was reduced after the priming stress (Figure S7d), likely

**FIGURE 2** Histone chaperone HIRA is enriched at stress-responsive genes after low-dose heat stress. (a) Venn diagram representing the overlap of HIRA binding sites from non-stressed and priming-stressed samples. (b) MA plots representing the mean peak intensity and the fold increase of each HIRA peak. Priming-stressed-specific (red), non-stressed-specific (blue), and overlapping (gray) peaks. (c) Identification of genomic locations of HIRA binding sites from non-stressed (left) and priming-stressed (right) samples. (d) HIRA binding frequency along a composite gene assembled from all coding genes. Gene length of the composite gene was calculated as arbitrary units, where the transcription start site (TSS) corresponds to 0 and the transcription termination site (TTS) corresponds to 100. (e) Frequency of ChIP-seq reads of HIRA, histone H3.3, histone H3, and control IgG around a composite of all HIRA peaks in non-stressed (left) and priming-stressed (right) cells. (f) Enriched canonical pathways for genes associated with prominent HIRA binding sites after a priming stress treatment. (g) Top binding motif sequences discovered within a window 250 nt upstream and downstream from the summit of HIRA peaks.

reflecting a nucleosome-depleted region, and the enrichment of histone variant H3.3 was normalized with the total H3 amount (Figures 3 and 4). Deposition of histone H3.3 is highly correlated with active transcription and related post-translational histone modifications (Wirbelauer et al., 2005). Consistently, we found that H3K4me3 and H3K9ac levels normalized to total H3 were significantly increased upon priming stress at the

TSS and the ORF of *HSPA1A*, but not at *GAPDH* (Figures 3e and S7e, note that the respective antibodies do not distinguish between canonical H3 and H3.3). Conversely, H3K4me and H3K4me2 at the *HSPA1A* locus were decreased or unchanged upon priming stress, respectively (Figure S7f,g). Prominent enrichments of HIRA, H3.3, and H3 modifications were also present at the TSS and ORF of *HSPA5*, another

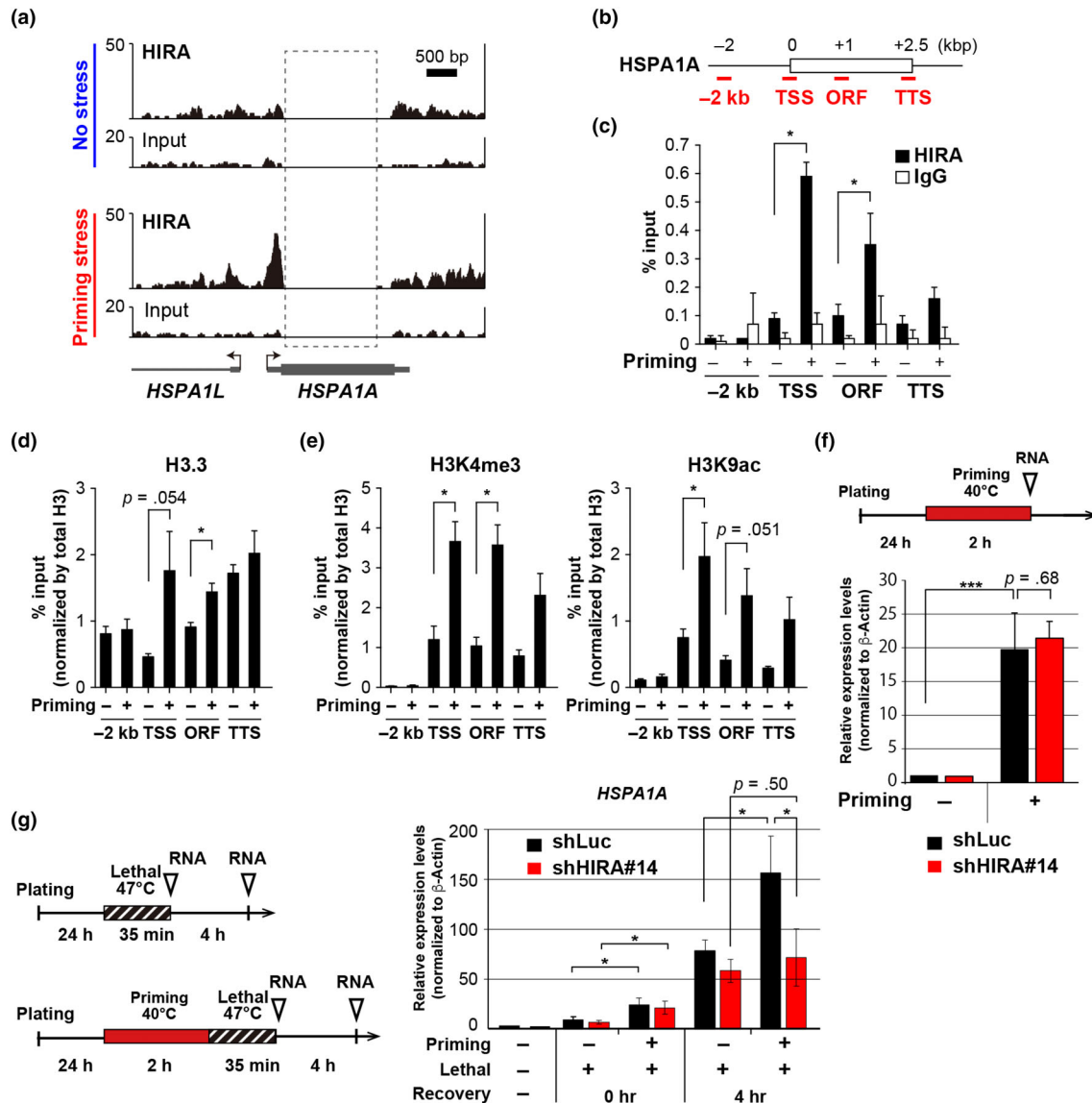


**FIGURE 3** HIRA and histone modifications are enriched at *HSPA1A* upon low-dose stress. (a) ChIP-seq profiles of HIRA at the *HSPA1A* locus in non-stressed and priming-stressed cells. Alignment of ChIP-seq reads was suppressed in the dashed-boxed region due to repetitive sequences within the genome. (b) qPCR primers for *HSPA1A*: -2 kb, approximately 2 kbp upstream of the TSS; TSS, transcription start site; ORF, open reading frame; TTS, transcription termination site. (c) ChIP-qPCR validation of HIRA enrichment at the *HSPA1A* locus. IgG, negative control IgG. (d and e) ChIP assay of histone H3.3 and indicated histone H3 modifications. (f) RT-qPCR analysis of *HSP70* mRNA expression after priming stress treatments in HIRA knockdown and control cells. Total RNA was harvested from cells with or without priming stress treatment. (g) RT-qPCR analysis of *HSP70* mRNA expression after lethal stress treatments in HIRA knockdown and control cells. Total RNA was harvested from cells immediately or 4 h after lethal stress treatment with or without priming stress. The expression levels were normalized to  $\beta$ -Actin expression levels and shown as relative values. The values in (c) to (g) represent the mean  $\pm$  S.D. derived from three independent experiments. A paired two-tailed *t*-test was applied for the statistical analysis. \*,  $p < .05$ ; \*\*\*,  $p < .005$ .

member of the HSP70 family whose expression was highly upregulated by priming stress (Figures S6a, S8b, and S9a–e). In concordance with the enrichment of active chromatin markers, RNA polymerase II and Med1, a component of the Mediator complex, were also enriched at the *HSPA1A* locus upon priming stress (Figures S7h,i), suggesting that this genomic locus was transcriptionally primed and/or activated by priming stress.

To investigate the role of the HIRA-H3.3 axis in resetting the epigenetic state of stress-responsive genes during heat stress acquired tolerance, we examined the mRNA levels of *HSPA1A* after stress treatments. We found that priming stress itself enhanced *HSPA1A* expression, and that HIRA knocked-down cells also showed the enhanced expression, suggesting that HIRA is not essential for the transcription of *HSPA1A* after priming stress (Figure 3f). Next, we examined the expression levels at

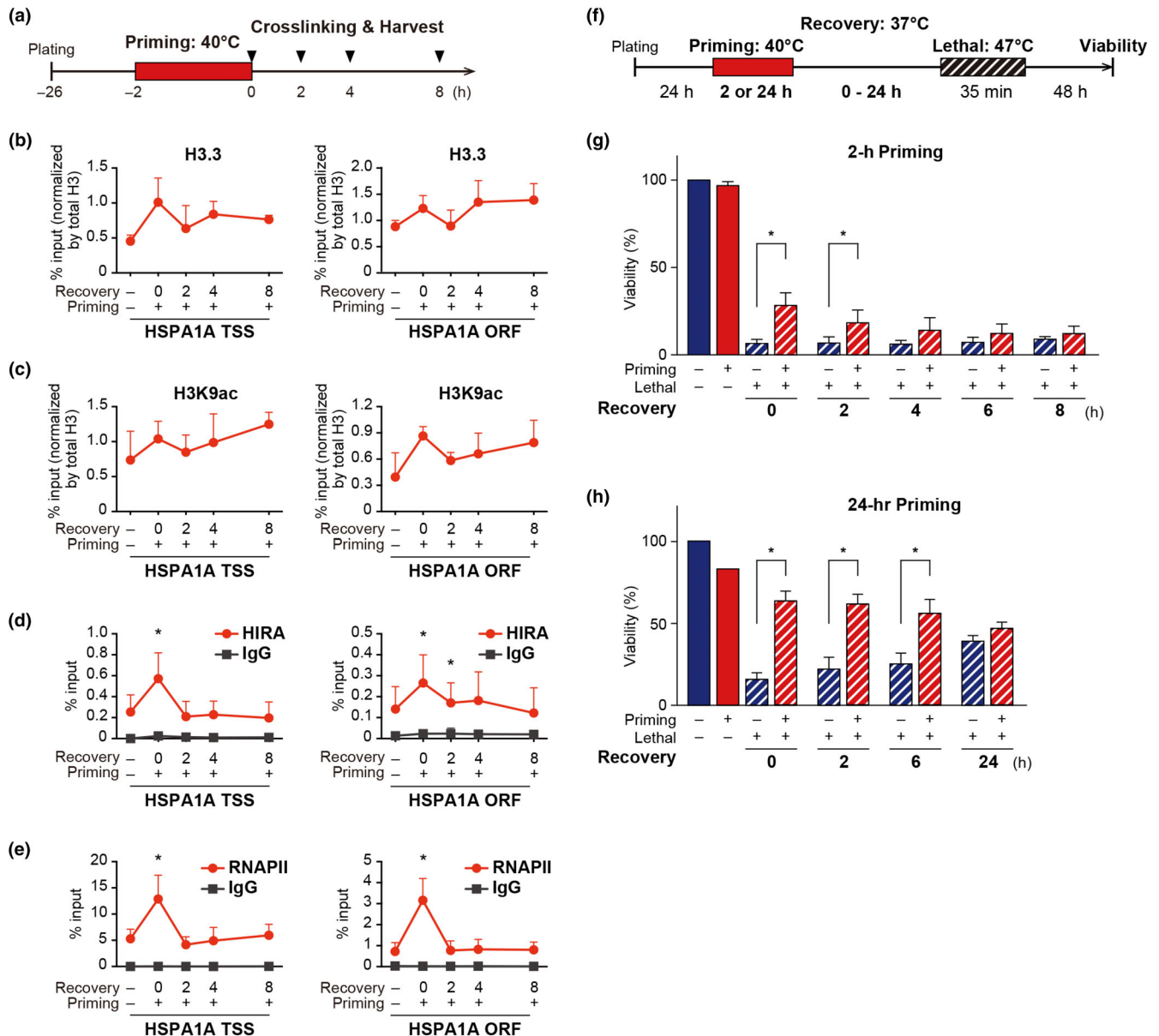


**FIGURE 4** Dynamics of chromatin changes after the priming stress. (a) Scheme of the ChIP assay with recovery time. After a priming stress, cells were allowed to recover at 37°C for the indicated time. (b–e) Time series analysis of the enrichment of histone H3.3 (b), H3K9ac (c), HIRA (d), and RNA polymerase II (e) at the TSS and the ORF of the *HSPA1A* locus after a priming stress. (f) Scheme of the acquired tolerance assay with recovery time. After priming heat stress, cells were allowed to recover at 37°C for 0–24 h, and were then treated with lethal heat stress. Cell viability was quantified 24 h after the lethal treatment using a Cell Counting Kit-8. (g and h) Cells were treated with a priming stress for 2 h (g) or for 24 h (h) and allowed to recover for the indicated time before lethal stress treatment. The values represent the mean  $\pm$  S.D. derived from three independent experiments. A paired two-tailed *t*-test was applied for the statistical analysis. \*,  $p < .05$ .

0 h and 4 h in a recovery period after applying the lethal stress alone (Priming  $-$ ), and the priming plus lethal stresses (P+L, Priming  $+$ ) (Figure 3g). We found that priming stress treatment enhanced *HSPA1A* expression at 0-h recovery time both in the control cells and the HIRA knocked-down cells. At 4-h recovery time after the lethal stress, however, P+L cells showed two-fold higher *HSPA1A* expression levels compared to L only cells in the control cells, but not in the HIRA knocked-down cells. These observations suggest that a preceding mild stress augments and maintains elevated *HSPA1A* expressions after the following lethal stress. Similar expression patterns were also observed in other HSP genes, *DNAJB1*, *HSPA4L*, and *HSPA5* (Figure S10a–f). Together, these results indicate that low-dose stress poises stress response genes for enhanced inducibility via the histone chaperone HIRA to prepare cells for a prospective and possibly harsh stress.

## 2.4 | HIRA is required to establish but not to maintain the transcription-permissive state of chromatin regions

The deposition of histone H3.3 onto chromatin can maintain genes in an active state, acting as an epigenetic memory (Kamada et al., 2018; Ng & Gurdon, 2008). Based on these reports, we asked whether it was possible that HIRA-mediated epigenetic changes at stress-responsive genes, including *HSPA1A*, after priming stress might be sustained over time, arming the cells with the ability to efficiently respond to prospective stresses for a finite time.

We found that H3.3 deposition and H3K9ac enrichment tended to persist over the course of 8 h after withdrawal of the priming stress, even though this tendency did not reach strict statistical significance (Figure 4a–c). In contrast, HIRA and RNA polymerase II occupancies were readily observed immediately after the priming stress treatment, but dropped to basal levels by approximately 2 h after the priming stress treatment (Figure 4d,e). When we measured the duration of acquired tolerance by varying the time between the priming and lethal stresses (Figure 4f), a 2-h priming stress enabled cells to maintain significant acquired tolerance for 2 h after the priming stress (Figure 4g). This phenotypic kinetics was shorter-lived than H3.3- and H3K9ac-occupancy at the *HSPA1A* TSS and ORF (Figure 4b,c), yet longer-lived than HIRA- and RNA polymerase II-occupancy at the same loci (Figure 4d,e), suggesting that HIRA is required for establishing but not maintaining a low-dose stress-induced primed chromatin state. A lack of exact correlation between the kinetics of acquired

tolerance and the particular epigenetic marks that we examined may imply that acquired tolerance-associated chromatin consists of other factors and/or conditions. Future studies may identify such factors.

Since cellular microenvironmental change may persist for a prolonged period, longer than just 2 h, we also investigated the effect of longer priming stress treatment. An extended priming stress treatment for 24 h conferred on cells significant and remarkably high tolerance (Figure 4h). Notably, the tolerance was sustained up to 6 h, which was longer than what we observed in the case of 2-h priming stress treatment (Figure 4g), suggesting that the epigenetic memory for the acquired tolerance persisted when cells were exposed to prolonged stimuli. It would be interesting to investigate in the future whether or not the residence of HIRA and H3.3 at the *HSPA1A* locus is accordingly prolonged in 24-h priming compared to 2-h priming.

## 3 | DISCUSSION

We have uncovered a novel role for human HIRA in a cellular response to low-dose stress. Mild stress triggers translocation of HIRA to stress-responsive genes, whereupon HIRA deposits histone H3.3 to cognate regions (Figure S11a). In parallel, nucleosome histones are modified (H3K4me3 and H3K9ac) to activate promoters and recruit RNA polymerase II. The recruitment of HIRA to the specific gene loci could be coupled with the activity of some transcription factors, such as AP-1 (Figure 2g). These low-dose stress responses enable cells to prepare for a subsequent severe stress, which constitutes a cellular hormetic response at the molecular level. We previously demonstrated that HIRA is required for acquired tolerance in fission yeast (Chujo et al., 2012; Tarumoto et al., 2013). It is impressive that the HIRA-dependent acquired tolerance is conserved among these phylogenetically diverse organisms, suggesting that it comprises an essential mechanism for eukaryotes to survive in the wildlife. It is known that the HIRA-H3.3 axis plays an important role in transcription recovery after UVC-induced DNA damages (Adam et al., 2013). It would be interesting to investigate in the future whether acquired tolerance responses are observed toward UVC-induced stresses in a HIRA-dependent manner.

To our surprise, *HIRA* knockdown did not affect *HSPA1A* expression induced by the priming stress alone (Figure 3f), suggesting that HIRA-mediated H3.3 deposition was not required for the immediate stress response per se. In response to the lethal stress alone, transcription was observed independently of HIRA at 0- and 4-h recovery (Figure 3g). However, we also found that the



*HSPA1A* expression level was significantly higher at the 4-h timepoint in recovery when the priming stress was applied prior to the lethal stress, compared to the lethal stress alone. Importantly, depletion of HIRA greatly diminished the P+L-specific elevated HSP expression at 4-h recovery. These results suggest that low-dose stress recruits the histone chaperone HIRA and histone H3.3 to stress-responsive genes to render them competent for immediate and effective expression upon encountering a harsher stress. We propose that the HIRA-H3.3 axis plays a unique role in stress resistance, namely arming cells to counter prospective severe stresses in response to mild stress.

We found that longer priming stresses increased the duration of active acquired tolerance in the recovery after the priming stresses (Figure 4h). As such, prolonged, and possibly frequent, weak stresses from fluctuating environmental conditions may elicit a strong and robust tolerance against forthcoming stresses. The tolerant state evoked by a priming stress could be maintained in the form of an active chromatin state, as histone variant H3.3 and some specific histone modifications, such as H3K4me3 and H3K36me3, are known to retain active gene states as an epigenetic memory, even between generations (Kamada et al., 2018; Kishimoto et al., 2017; Ng & Gurdon, 2008). Alternatively, proteins de novo produced by the priming stress, such as HSP70, may contribute to the maintenance of the acquired tolerance conditions. Thirdly, it is possible that the poised state of the genes involved in the eIF2 signaling and hypoxia signaling pathways play a role in the maintenance. Further studies are required to dissect the molecular machinery of transient memory of acquired tolerance.

As befits a biological system, the HIRA-dependent acquired tolerance is transient rather than permanent. The transient acquired tolerance is adaptive because the poised state of stress-response genes costs extra-resources, which is diverted from the cellular budget for other vital cell activities. Accordingly, the epigenetic state should be allowed to return to basal levels if environmental conditions normalize. During this time window, however, the poised epigenetic state of acquired tolerance can lead to a robust response if conditions suddenly worsen. In a real-world scenario, it appears that the transient nature of acquired tolerance limits its effects in normal tissues under strong homeostatic control, where fluctuations of stress above threshold levels would rarely occur. However, it is not the case in various pathologies including cancers.

Blood flow rate within tumors, unlike that in normal tissues, frequently changes both spatially and temporally, leading to fluctuations of local oxygen pressure (reviewed in [Gillies et al., 2012]). It is possible that the fluctuation of microenvironmental conditions is not limited to

oxygen, but involves other factors such as local pH, glucose, inflammatory cytokines, and tissue pressure (Figure S11b). As a result, cancer cells may be constitutively equipped with general stress resistance via, for example, induced heat shock proteins, which are expressed at high levels in various types of cancer cells and play a role in tumor growth and resistance to anticancer therapy (Kim et al., 2011; Pocaly et al., 2007; Rohde et al., 2005). Alternatively, the effect may be specific, such as VEGFR1 expression through HIRA-dependent incorporation of acetylated histone H3.3 at the cognate locus (Dutta et al., 2010). These general and specific effects together could provide cancer cells with resistance to lethal stresses including cytotoxic chemotherapeutics. In this setting, it is worth investigating whether HIRA-dependent acquired tolerance is implicated in cancer survival, acquired drug resistance, and progression.

## 4 | EXPERIMENTAL PROCEDURES

### 4.1 | Cell culture

WI-38 human lung fibroblast cells were immortalized by expressing human TERT. Primary and immortalized WI-38, IMR-90, HeLa, and 293T cells were grown at 37°C and 5% CO<sub>2</sub> in Dulbecco's modified Eagle's medium (DMEM) (Nissui) supplemented with 10% FBS (GIBCO), L-glutamine, and antibiotics.

### 4.2 | Heat treatment

Cells were seeded at a density of  $1.1 \times 10^4$  or  $1.7 \times 10^4$  cells/cm<sup>2</sup> in 35 mm dishes for immortalized cells and primary cells, respectively, and incubated for 24 h at 37°C before heat shock treatment. For priming stress treatment, culture media was replaced with fresh media preheated at 40°C, and cells were cultured in an incubator at 40°C ( $\pm 0.5^\circ\text{C}$ ) and 5% CO<sub>2</sub> for 2 h. For lethal stress treatment, culture media was replaced with fresh media preheated at 47°C, and cells were cultured in an incubator at 47°C ( $\pm 0.5^\circ\text{C}$ ) and 5% CO<sub>2</sub> for 35 min. After heat treatment, the media was replaced by fresh media (37°C), and the cells were incubated in an incubator at 37°C ( $\pm 0.5^\circ\text{C}$ ) and 5% CO<sub>2</sub> for 48 h. Cell viability was quantified using a Cell Counting Kit-8 (Dojindo) and SpectraMax 340 Microplate Reader (Molecular Devices).

### 4.3 | shRNA transfection

shHIRA#14 (5'-GCTAACTTGTAATATTGAA-3') and shControl (5'-CCAATGCTTTGATGCCAAA-3') duplex

oligonucleotide cassettes were cloned into a doxycycline-inducible lentiviral RNAi vector, pCII-U6tet-shRNA-EF-TetR-IRES-puro. To induce shRNA expression, doxycycline was added to the culture media (1 µg/ml) at least 6 days prior to each experiment. shHIRA#2 (5'-GGAGATGACAACTGATTA-3') and shLuciferase (5'-TAAGGCTATGAAGAGATAC-3') cassettes were cloned into a conventional lentiviral RNAi vector, pCII-RNAi-MCS-CMV-puro. These lentiviral vectors were a generous gift from Dr. Shin Yonehara, Kyoto University. For packaging, 293T cells were transfected with lentiviral vectors using the calcium phosphate method. Culture supernatants were supplemented with 5 µg/mL polybrene (Sigma-Aldrich) and incubated with target cells. Infected cells were selected by incubating with 2.5 µg/mL puromycin (Sigma-Aldrich) for 3 days.

#### 4.4 | Microarray analysis

Total RNA from HIRA knockdown and control cells was analyzed with a GeneChip Human Gene 2.0 ST Array (Affymetrix) according to the manufacturer's instructions. After using the RMA algorithm to obtain the summarized probeset-level expression data, the array data were transferred to GeneSpring microarray analysis software (Agilent Technologies) for normalization and calculation of the fold change.

#### 4.5 | Chromatin immunoprecipitation (ChIP) and quantitative PCR

ChIP was performed essentially as described (Yoshida et al., 2015), with some modifications. Cells were cross-linked with 1% formaldehyde for 8 min at room temperature and quenched with 125 mM glycine for 3 min. Fixed cells were washed twice with ice-cold PBS and then lysed successively in Lysis Buffer 1 (50 mM HEPES-KOH, pH 7.4, 140 mM NaCl, 1 mM EDTA, 10% Glycerol, 0.5% NP-40, 0.25% Triton-X-100, 1 mM PMSF), Lysis Buffer 2 (20 mM Tris-HCl, pH 8.0, 200 mM NaCl, 1 mM EDTA, 0.5 mM EGTA, 1 mM PMSF), Lysis Buffer 3-150NaCl (20 mM Tris-HCl, pH 7.5, 150 mM NaCl, 1 mM EDTA, 0.5 mM EGTA, 1% Triton-X-100, 0.1% Sodium deoxycholate [Sigma-Aldrich], 0.1% SDS, protease inhibitor cocktail [Roche]) and Lysis Buffer 3-500NaCl (20 mM Tris-HCl, pH 7.5, 500 mM NaCl, 1 mM EDTA, 0.5 mM EGTA, 1% Triton-X-100, 0.1% Sodium deoxycholate, 0.1% SDS, protease inhibitor cocktail), in that order. The lysates were sonicated using a Branson Sonifier 250 at 4°C to generate DNA fragments of 100–500 bp, clarified by centrifugation (15,000 rpm for 15 min at 4°C) and

then incubated overnight at 4°C with beads (Dynabeads M-280 sheep anti-rabbit IgG or anti-mouse IgG, or Dynabeads sheep anti-rat IgG [Invitrogen]) that had been pre-blocked with 0.5% BSA and mixed with the indicated primary antibodies. To remove nonspecifically bound proteins, beads were washed five times with RIPA Buffer (50 mM HEPES-KOH, pH 7.4, 500 mM LiCl, 1 mM EDTA, 1% NP-40, 0.7% sodium deoxycholate) and once with TE Buffer (50 mM Tris-HCl, pH 8.0, 10 mM EDTA). The DNA-protein complex was eluted from the beads in Elution Buffer (50 mM Tris-HCl, pH 8.0, 10 mM EDTA, 1% SDS) for 20 min at 65°C, and de-crosslinked overnight at 65°C. The eluted samples were then treated with RNase A and proteinase K, and purified using a PCR purification kit (QIAGEN). Quantitative PCR was performed with Power SYBR Green PCR Master Mix (Applied Biosystems) in an ABI StepOnePlus Real-Time PCR System (Applied Biosystems). The results are presented as the percentage of the input chromatin enriched by the ChIP procedure, or as the normalized enrichment with respect to the ChIP efficiency for total H3 (for analysis of H3.3 and modifications). The primer sets used in this study are listed in Table S1. Antibodies used for ChIP assays were: normal rabbit IgG (Santa Cruz, sc-2027), normal mouse IgG (Santa Cruz, sc-2025), normal rat IgG (Santa Cruz, sc-2026), anti-histone H3 (Abcam, ab1791), anti-H3.3 (Cosmo bio, CE-040B), anti-RNA Polymerase II clone CTD4H8 (Millipore, 05-623), and anti-MED1 (BETHYL, A300-793A). A rabbit polyclonal antibody to human HIRA was raised in our laboratory using a recombinant HIRA peptide (421-729 amino acids from human HIRA) as an antigen. Anti-H3K4me, anti-H3K4me2, anti-H3K4me3 and anti-H3K9ac were prepared and provided by Dr. Hiroshi Kimura (Tokyo Institute of Technology [Kimura et al., 2008]).

#### 4.6 | ChIP-seq and data analysis

ChIP-seq libraries were prepared from ChIP-DNA or input DNA using a NEBNext ChIP-seq Library kit (New England Biolabs) according to the manufacturer's instructions. The resulting libraries were sequenced with a HiSeq 2000 DNA sequencer (Illumina). The overall read quality was checked using FastQC v0.11.3. A total of approximately 45 million sequenced reads were mapped to the human genome (UCSC, hg19) using Bowtie v1.1.1 alignment software (Langmead et al., 2009), allowing only unique reads mapped to a single location with no more than two mismatches. Information and statistics for the sequencing and mapping are summarized in Tables S2 and S3. DROMPA2 v2.6.4 software (Nakato et al., 2013) with its default settings ( $p < 0.001$  and FDR

< 0.01 for ChIP/Input enrichment for each 100-bp bin) was used to call peaks representing enriched binding sites. Peaks were visualized using the IGV genome browser v2.3.57 (Robinson et al., 2011).

#### 4.7 | MA plots

All ChIP-seq peaks were classified into three groups: priming-stress-specific peaks, non-stress-specific peaks, and overlapping peaks. Overlapping peaks were defined by an intersection of the peaks from two conditions by at least 1 base pair. The ( $M$ ,  $A$ ) values of all peaks were calculated with DROMPA2 and plotted, where the  $\log_2$  ratio of read density between two conditions  $M = \log_2$  (read density in Priming stress/read density in No stress), and the average  $\log_2$  read density  $A = 0.5 \times \log_2$  (read density in Priming stress  $\times$  read density in No stress).

#### 4.8 | Annotation and genomic distribution

Peaks were annotated with neighboring genes (maximum distance between a peak and an annotated gene was 2000 bp) using the refFlat file from UCSC Genome Browser, allowing a peak to gain multiple gene annotations. All annotated peaks were categorized according to the genomic features, including 5'UTR, 3'UTR, exons, introns, and intergenic regions (outside of these defined regions). DROMPA2 was used to generate the average read distribution around coding genes.

#### 4.9 | Pathway analysis

For pathway analysis of ChIP-seq data, peaks located within a region 2000 bp upstream and downstream from TSSs and with significant  $M$  values in MA plots ( $p < 0.05$  in a binomial test by DROMPA2) were selected. Among priming-stress-specific peaks, approximately 2000 peaks with high  $M$  values were further selected, as up to 2000 entities could be accepted in a single pathway analysis in Ingenuity Pathway Analysis (QIAGEN).

#### 4.10 | GO enrichment analysis

For GO enrichment analysis of RNA-seq data, differentially expressed genes (DEGs) were selected and uploaded in the online analysis tool DAVID Bioinformatics Resources (v6.8).

#### 4.11 | Motif discovery based on ChIP-seq data

Nucleotide sequences underlying the peaks from HIRA ChIP-seq data were extracted with a window 250 nt upstream and downstream of the summit of each HIRA peak. Sequences were submitted to the MEME-ChIP analysis tool (MEME Suite v5.0.3) for motif discovery (Bailey et al., 2009). Motif sequences with 6–30 nt were used for analysis.

#### 4.12 | Immunoblots

Cell pellets were lysed in  $2 \times$  SDS sample buffer (125 mM Tris, 4% SDS, 20% Glycerol, 4% 2-mercaptoethanol, pH 6.8). Protein samples were separated by SDS-PAGE, and transferred onto a PVDF membrane (Millipore). After blocking in 3% BSA or Blocking One (Nacalai) at room temperature, the blots were immunostained with the indicated antibodies. Respective proteins were detected with horseradish peroxidase-linked secondary antibodies (GE Healthcare) and ECL reagents (GE Healthcare) according to the manufacturer's instructions. Antibodies used for immunoblots were: anti-HIRA (Active motif, 39557), in-house anti-HIRA, anti-histone H3.1 (Cosmo bio, CE-039B), anti-histone H3.3 (Cosmo bio, CE-040B), anti-H3 (ab1791), anti-H2A (Abcam, ab177308), anti-HA (BaBCo, MMS101R) and anti-actin (Millipore, MAB1501R).

#### 4.13 | RNA isolation and RT-PCR

Total RNA from cultured cells was extracted using an RNeasy Mini kit (QIAGEN) with on-column DNase I digestion following the manufacturer's protocol. The cDNA was prepared from 1  $\mu$ g of total RNA using AMV reverse-transcriptase XL (TaKaRa) and oligo dT primers, and then subjected to real-time PCR as described for ChIP analyses. The primer sets used for RT-PCR are listed in Table S4.

#### 4.14 | Quantification and statistical analysis

As indicated in the figure legends, data values reported in the figures are the mean  $\pm$  standard deviation calculated using Microsoft Excel. For statistical analysis in the comparison of cellular viability and ChIP efficiency, a paired two-tailed Student's  $t$ -test in Microsoft Excel was used.

## AUTHOR CONTRIBUTIONS

Y Nagagaki: conceptualization, formal analysis, funding acquisition, investigation, writing—original draft, review, and editing. Y Kozakura: data curation, formal analysis, visualization. T Mahandaran: writing—review and editing. Y Fumoto: investigation. R Nakato: data curation, formal analysis, resources, software, visualization. K Shirahige: resources. F Ishikawa: conceptualization, funding acquisition, supervision, writing—original draft, review, and editing.

## ACKNOWLEDGMENTS

We thank Drs. James A. Hejna and Peter M. Carlton (Kyoto University Graduate School of Biostudies) for critical reading of the manuscript. This research was supported by the Project for Cancer Research and Therapeutic Evolution (P-CREATE) Grant Number 21cm0106113h0006 from the Japan Agency for Medical Research and Development (AMED) (to F. Ishikawa), MEXT KAKENHI Grant Numbers 15H02383 and 25134710 (to F. Ishikawa), Research Grant from Princess Takamatsu Cancer Research Fund (to F. Ishikawa), Research Grant from The Uehara Memorial Foundation (202220433 to F. Ishikawa), Grant-in-Aid for JSPS Research Fellow 14J08310 (to Y. Nagagaki), and the Core-to-Core Program (JPJSCCA20200009) from the Japan Society for the Promotion of Science (JSPS).

## CONFLICT OF INTEREST STATEMENT

The authors declare that they have no conflicts of interest.

## DATA AVAILABILITY STATEMENT

Plasmids and antibodies generated in this study can be obtained by contacting the lead contact. ChIP-seq data for HIRA and Histone H3.3 have been deposited into the Sequence Read Archive database under the accession number SRP098615 and the Gene Expression Omnibus database under the accession number GSE253873, respectively. Microarray data and RNA-seq data reported are available in the Gene Expression Omnibus database under the accession numbers GSE252837 and GSE253874, respectively.

## ORCID

Yoshikazu Nagagaki  <https://orcid.org/0009-0005-7865-1158>

Theventhiran Mahandaran  <https://orcid.org/0000-0002-7874-7687>

Fuyuki Ishikawa  <https://orcid.org/0000-0002-5580-2305>

## REFERENCES

- Adam, S., Polo, S. E., & Almouzni, G. (2013). Transcription recovery after DNA damage requires chromatin priming by the H3.3 histone chaperone HIRA. *Cell*, *155*(1), 94–106. <https://doi.org/10.1016/j.cell.2013.08.029>
- Ahmad, K., & Henikoff, S. (2002). The histone variant H3.3 marks active chromatin by replication-independent nucleosome assembly. *Mol Cell*, *9*(6), 1191–1200. [https://doi.org/10.1016/S1097-2765\(02\)00542-7](https://doi.org/10.1016/S1097-2765(02)00542-7)
- Bailey, T. L., Boden, M., Buske, F. A., Frith, M., Grant, C. E., Clementi, L., & Noble, W. S. (2009). MEME SUITE: tools for motif discovery and searching. *Nucleic Acids Res*, *37*(Web Server issue), W202–W208. <https://doi.org/10.1093/nar/gkp335>
- Banaszynski, L. A., Wen, D., Dewell, S., Whitcomb, S. J., Lin, M., Diaz, N., Elsasser, S. J., Chappier, A., Goldberg, A. D., Canaani, E., et al. (2013). Hira-dependent histone H3.3 deposition facilitates PRC2 recruitment at developmental loci in ES cells. *Cell*, *155*(1), 107–120. <https://doi.org/10.1016/j.cell.2013.08.061>
- Calabrese, V., Cornelius, C., Cuzzocrea, S., Iavicoli, I., Rizzarelli, E., & Calabrese, E. J. (2011). Hormesis, cellular stress response and vitagenes as critical determinants in aging and longevity. *Mol Aspects Med*, *32*(4-6), 279–304. <https://doi.org/10.1016/j.mam.2011.10.007>
- Chujo, M., Tarumoto, Y., Miyatake, K., Nishida, E., & Ishikawa, F. (2012). HIRA, a conserved histone chaperone, plays an essential role in low-dose stress response via transcriptional stimulation in fission yeast. *J Biol Chem*, *287*(28), 23440–23450. <https://doi.org/10.1074/jbc.M112.349944>
- Dirnagl, U., Becker, K., & Meisel, A. (2009). Preconditioning and tolerance against cerebral ischaemia: from experimental strategies to clinical use. *Lancet Neurol*, *8*(4), 398–412. [https://doi.org/10.1016/S1474-4422\(09\)70054-7](https://doi.org/10.1016/S1474-4422(09)70054-7)
- Dutta, D., Ray, S., Home, P., Saha, B., Wang, S., Sheibani, N., & Paul, S. (2010). Regulation of angiogenesis by histone chaperone HIRA-mediated incorporation of lysine 56-acetylated histone H3.3 at chromatin domains of endothelial genes. *J Biol Chem*, *285*(53), 41567–41577. <https://doi.org/10.1074/jbc.M110.190025>
- Gems, D., & Partridge, L. (2008). Stress-response hormesis and aging: “that which does not kill us makes us stronger”. *Cell Metab*, *7*(3), 200–203. <https://doi.org/10.1016/j.cmet.2008.01.001>
- Gillies, R. J., Verduzco, D., & Gatenby, R. A. (2012). Evolutionary dynamics of carcinogenesis and why targeted therapy does not work. *Nat Rev Cancer*, *12*, 487–493. <https://doi.org/10.1038/nrc3298>
- Goldberg, A. D., Banaszynski, L. A., Noh, K. M., Lewis, P. W., Elsasser, S. J., Stadler, S., & Allis, C. D. (2010). Distinct factors control histone variant H3.3 localization at specific genomic regions. *Cell*, *140*(5), 678–691. <https://doi.org/10.1016/j.cell.2010.01.003>
- Heusch, G. (2013). Cardioprotection: chances and challenges of its translation to the clinic. *Lancet*, *381*(9861), 166–175. [https://doi.org/10.1016/S0140-6736\(12\)60916-7](https://doi.org/10.1016/S0140-6736(12)60916-7)
- Jin, C., & Felsenfeld, G. (2006). Distribution of histone H3.3 in hematopoietic cell lineages. *Proc Natl Acad Sci U S A*, *103*(3), 574–579. <https://doi.org/10.1073/pnas.0509974103>

- Kamada, R., Yang, W., Zhang, Y., Patel, M. C., Yang, Y., Ouda, R., & Ozato, K. (2018). Interferon stimulation creates chromatin marks and establishes transcriptional memory. *Proc Natl Acad Sci U S A*, *115*(39), E9162–e9171. <https://doi.org/10.1073/pnas.1720930115>
- Kim, H., Heo, K., Choi, J., Kim, K., & An, W. (2011). Histone variant H3.3 stimulates HSP70 transcription through cooperation with HP1gamma. *Nucleic Acids Res*, *39*(19), 8329–8341. <https://doi.org/10.1093/nar/gkr529>
- Kimura, H., Hayashi-Takanaka, Y., Goto, Y., Takizawa, N., & Nozaki, N. (2008). The organization of histone H3 modifications as revealed by a panel of specific monoclonal antibodies. *Cell Struct Funct*, *33*(1), 61–73. <https://doi.org/10.1247/csf.07035>
- Kirov, N., Shtilbans, A., & Rushlow, C. (1998). Isolation and characterization of a new gene encoding a member of the HIRA family of proteins from *Drosophila melanogaster*. *Gene*, *212*(2), 323–332. [https://doi.org/10.1016/S0378-1119\(98\)00143-7](https://doi.org/10.1016/S0378-1119(98)00143-7)
- Kishimoto, S., Uno, M., Okabe, E., Nono, M., & Nishida, E. (2017). Environmental stresses induce transgenerationally inheritable survival advantages via germline-to-soma communication in *Caenorhabditis elegans*. *Nat Commun*, *8*, 14031. <https://doi.org/10.1038/ncomms14031>
- Langmead, B., Trapnell, C., Pop, M., & Salzberg, S. L. (2009). Ultrafast and memory-efficient alignment of short DNA sequences to the human genome. *Genome Biol*, *10*(3), R25. <https://doi.org/10.1186/gb-2009-10-3-r25>
- Lorch, Y., & Kornberg, R. D. (2015). Chromatin-remodeling and the initiation of transcription. *Q Rev Biophys*, *48*(4), 465–470. <https://doi.org/10.1017/S0033583515000116>
- Nakato, R., Itoh, T., & Shirahige, K. (2013). DROMPA: easy-to-handle peak calling and visualization software for the computational analysis and validation of ChIP-seq data. *Genes Cells*, *18*(7), 589–601. <https://doi.org/10.1111/gtc.12058>
- Ng, R. K., & Gurdon, J. B. (2008). Epigenetic memory of an active gene state depends on histone H3.3 incorporation into chromatin in the absence of transcription. *Nat Cell Biol*, *10*(1), 102–109. <https://doi.org/10.1038/ncb1674>
- Pchelintsev, N. A., McBryan, T., Rai, T. S., van Tuyn, J., Ray-Gallet, D., Almouzni, G., & Adams, P. D. (2013). Placing the HIRA histone chaperone complex in the chromatin landscape. *Cell Rep*, *3*(4), 1012–1019. <https://doi.org/10.1016/j.celrep.2013.03.026>
- Pocaly, M., Lagarde, V., Etienne, G., Ribeil, J. A., Claverol, S., Bonneau, M., & Pasquet, J. M. (2007). Overexpression of the heat-shock protein 70 is associated to imatinib resistance in chronic myeloid leukemia. *Leukemia*, *21*(1), 93–101. <https://doi.org/10.1038/sj.leu.2404463>
- Rai, T. S., Cole, J. J., Nelson, D. M., Dikovskaya, D., Faller, W. J., Vizioli, M. G., & Adams, P. D. (2014). HIRA orchestrates a dynamic chromatin landscape in senescence and is required for suppression of neoplasia. *Genes Dev*, *28*(24), 2712–2725. <https://doi.org/10.1101/gad.247528.114>
- Rai, T. S., Puri, A., McBryan, T., Hoffman, J., Tang, Y., Pchelintsev, N. A., & Adams, P. D. (2011). Human CABIN1 is a functional member of the human HIRA/UBN1/ASF1a histone H3.3 chaperone complex. *Mol Cell Biol*, *31*(19), 4107–4118. <https://doi.org/10.1128/MCB.05546-11>
- Ray-Gallet, D., Quivy, J. P., Scamps, C., Martini, E. M., Lipinski, M., & Almouzni, G. (2002). HIRA is critical for a nucleosome assembly pathway independent of DNA synthesis. *Mol Cell*, *9*(5), 1091–1100. [https://doi.org/10.1016/S1097-2765\(02\)00526-9](https://doi.org/10.1016/S1097-2765(02)00526-9)
- Robinson, J. T., Thorvaldsdottir, H., Winckler, W., Guttman, M., Lander, E. S., Getz, G., & Mesirov, J. P. (2011). Integrative genomics viewer. *Nat Biotechnol*, *29*, 24–26. doi:10.1038/nbt.1754
- Rohde, M., Daugaard, M., Jensen, M. H., Helin, K., Nylandsted, J., & Jaattela, M. (2005). Members of the heat-shock protein 70 family promote cancer cell growth by distinct mechanisms. *Genes Dev*, *19*(5), 570–582. <https://doi.org/10.1101/gad.305405>
- Tagami, H., Ray-Gallet, D., Almouzni, G., & Nakatani, Y. (2004). Histone H3.1 and H3.3 complexes mediate nucleosome assembly pathways dependent or independent of DNA synthesis. *Cell*, *116*(1), 51–61. [https://doi.org/10.1016/S0092-8674\(03\)01064-X](https://doi.org/10.1016/S0092-8674(03)01064-X)
- Tarumoto, Y., Kanoh, J., & Ishikawa, F. (2013). Receptor for activated C-kinase (RACK1) homolog Cpc2 facilitates the general amino acid control response through Gcn2 kinase in fission yeast. *J Biol Chem*, *288*(26), 19260–19268. <https://doi.org/10.1074/jbc.M112.445270>
- Wirbelauer, C., Bell, O., & Schubeler, D. (2005). Variant histone H3.3 is deposited at sites of nucleosomal displacement throughout transcribed genes while active histone modifications show a promoter-proximal bias. *Genes Dev*, *19*(15), 1761–1766. <https://doi.org/10.1101/gad.347705>
- Yoshida, K., Maekawa, T., Zhu, Y., Renard-Guillet, C., Chatton, B., Inoue, K., & Ishii, S. (2015). The transcription factor ATF7 mediates lipopolysaccharide-induced epigenetic changes in macrophages involved in innate immunological memory. *Nat Immunol*, *16*(10), 1034–1043. <https://doi.org/10.1038/ni.3257>

## SUPPORTING INFORMATION

Additional supporting information can be found online in the Supporting Information section at the end of this article.

**How to cite this article:** Nagasaki, Y., Kozakura, Y., Mahandaran, T., Fumoto, Y., Nakato, R., Shirahige, K., & Ishikawa, F. (2024). Histone H3.3 chaperone HIRA renders stress-responsive genes poised for prospective lethal stresses in acquired tolerance. *Genes to Cells*, *29*(9), 722–734. <https://doi.org/10.1111/gtc.13140>